

## Strain Evolution in Coherent Ge/Si Islands

Chuan-Pu Liu,<sup>1,\*</sup> J. Murray Gibson,<sup>1</sup> David G. Cahill,<sup>1</sup> Theodore I. Kamins,<sup>2</sup> David P. Basile,<sup>2</sup> and R. Stanley Williams<sup>2</sup>

<sup>1</sup>Materials Research Laboratory, University of Illinois at Urbana-Champaign, 104 South Goodwin Avenue, Urbana, Illinois 61801

<sup>2</sup>Hewlett-Packard Laboratories, P.O. Box 10350, Palo Alto, California 94303-0867

(Received 24 May 1999)

Strain evolution of coherent Ge islands on Si(001) is measured using a newly developed transmission electron microscopy technique based on two-beam dark-field strain imaging. The strain measurements show that a metastable Ge island shape is involved in the shape transition between pyramids and domes; this shape is more readily observed for growth at 550 than 600 °C because of the slower rate at which islands cross the kinetic barrier between shapes. The strain relaxation changes discontinuously between pyramids and domes, indicating that the underlying shape transition is first order.

PACS numbers: 68.35.Bs, 61.16.Bg, 68.35.Rh

Ge on Si(001) is a model system that forms coherently strained islands above the surface after a wetting layer of approximately 3 equivalent monolayers (1 eq-ML =  $6.3 \times 10^{14}$  atoms/cm<sup>2</sup>) has been deposited. Islands of small volume are typically square-based pyramids bounded by {105} facets; larger volume islands transform to a dome shape with a complex geometry of steeper facets. Strain governs this shape transition, which leads to a bimodal size distribution [1,2]. Size and shape selection in strained epitaxial islands (“quantum dots”) is a subject of considerable interest [3–6]. However, no strain measurements have ever been made in detail to understand the role of strain in the shape transition.

In this paper, we measure strain in individual islands within a population of islands for different growth conditions using a novel transmission electron microscopy (TEM) technique. Since strain is a first-order thermodynamic parameter, by measuring the strain evolution, we examine the energetics of the shape transition of Ge islands on Si(001). Our results show that there are three characteristic strain levels associated with three major island populations. We identify the type of island with the intermediate strain level as a metastable shape between pyramids and domes. This metastable shape is not thermodynamically preferred, but it acts as a kinetic intermediate for the transformation of pyramids to domes. In addition, we show that the change in strain among these three different types of islands is discontinuous, suggesting that the underlying shape transformation is first order.

Our new strain measurement technique using TEM is based on the strain-induced phase shift,  $2\pi\mathbf{g} \cdot \mathbf{R}$  [7], where  $\mathbf{g}$  is the vector of the operating Bragg reflection and  $\mathbf{R}$  is the lattice displacement. Relaxation of the coherently strained Ge islands from the in-plane lattice spacing for Si(001) produces fringes in the images with intensity maxima separated by  $2\pi\mathbf{g} \cdot \mathbf{R}$ . We have shown that the complicated strain field in a coherent island can be simplified and the position of each fringe and the numbers of fringes present in either lobe of a two-beam TEM image for an island are strongly related to the strain in the

island [7,8]. Consequently, the strain can be determined independent of any specific model and the accuracy of this technique can be better than 10% [8]. We measure the strain by relating the outermost fringe spacing inside the island to the total phase shift:

$$2\pi\mathbf{g} \cdot \mathbf{R} = 2\pi\mathbf{g} \cdot \varepsilon x = \left(n - \frac{1}{2}\right)\pi, \quad (1)$$

where  $\varepsilon$  is the local strain,  $x$  is the fringe position, and  $n$  is the fringe number. Thus, this technique measures the average strain in the islands with respect to the Si lattice, which is quantitatively equivalent to the average strain *relaxation* of the Ge islands (for a maximum possible relaxation of 4.2% to the bulk lattice constant of Ge).

Using Eq. (1), we measure the average strain as a function of the island diameter for each growth or annealing condition. With this information, we are able to gain insight into the thermodynamic stability of the sample by correlating the strain with each island shape; this microscopic information is not available in techniques that measure only the average strain of all islands, e.g., x-ray diffraction [9] or wafer bending [10], or that measure only the shape of individual islands, e.g., atomic force microscopy or scanning tunneling microscopy.

Two sets of samples are analyzed. The first set is a series of Ge films deposited on Si(001) for various times by chemical vapor deposition at 600 °C and 10 Torr; the deposition rate is  $\sim 6$  eq-ML min<sup>-1</sup>. In the second set, Ge films are deposited on Si(001) at 550 °C to a thickness of 8 eq-ML using the same growth process as in the first set, and the samples are subsequently annealed for varying lengths of time at 550 °C. Further details of the samples can be found in Refs. [11] and [12]. TEM plan-view thin foils are prepared by mechanical thinning to 30  $\mu\text{m}$  in thickness, followed by Ar<sup>+</sup> ion thinning the back side only until the sample is perforated. Images are acquired digitally using a slow-scan CCD camera in a Philips CM12 operating at 120 keV. Native oxide is measured to be  $\approx 2$  nm thick by an ellipsometer and so the consumption

of the deposited Ge is less than 1 nm [13]. Thereby, since even the smallest Ge islands are  $\sim 2$  nm tall, we expect that the effect of the oxide layer on strain measurement and shape determination is insignificant.

The dark-field images of strain contrast of Ge islands on Si(001) are acquired in relatively thick regions ( $t \sim 0.6 \mu\text{m}$ ) using the exact two-beam condition for the 400 g vector. Under this imaging condition, pyramids and domes can be easily distinguished by the image shape from strain contrast [14], as shown in Fig. 1(a), where the shape looks curved at the island center for pyramids compared to straight line for domes. In the set of the samples grown at 600 °C, only pyramids with a wide size distribution occur for the 6 eq-ML Ge film. Domes subsequently form and represent 50% of the total islands for the 9 eq-ML layer and almost 100% for the 14 eq-ML layer. In the annealing experiment at 550 °C, both pyramids and domes coexist initially for the as-deposited sample. The mean island volume and the total volume of the islands increase, and the areal island density decreases for both the pyramids and domes for the first 10 min of annealing as Ge moves from the wetting layer into the islands [12], but the ratio of the areal densities of pyramids to domes and the total volume of the islands remain approximately stable from 10 to 80 min [12].

Regarding the strain measurement, we are concerned with the fringe features confined inside an island in a strain-contrast image. For pyramids, the numbers of fringes present in either side of the islands are always

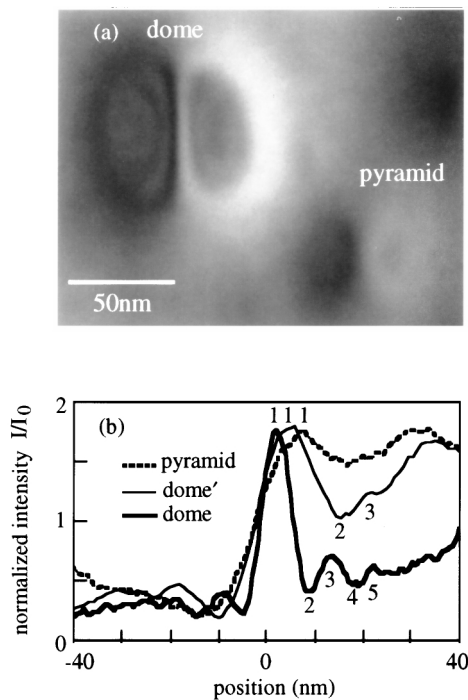


FIG. 1. Dark-field images of a pyramid and a dome using  $g = 400$ . (b) Line traces across three typical islands found in the experiment, where the fringes on one side of the images are numbered.

less than two for all growth conditions, implying that the strain of pyramids is independent of growth or annealing conditions. Analysis of the larger pyramids using Eq. (1) gives a strain value of about 0.5%. However, for domelike shapes, the numbers of fringes and the corresponding fringe spacing critically depend on the growth or the annealing conditions, as demonstrated in Fig. 1(b). For example, while only three fringes occur for domes annealed for 5 min [dome' in Fig. 1(b)], five fringes are present for domes annealed for 80 min. The average strains of these two dome-shaped islands in Fig. 1(b) are measured to be about 1% and 2%. The strain-contrast TEM images directly reveal that strain remains fairly constant for pyramids but varies dramatically for dome-like islands, even though the distribution of domelike diameters is narrower.

Figure 2 shows our central results: the strain evolution of Ge islands on Si(001) for 6, 9, and 14 eq-ML

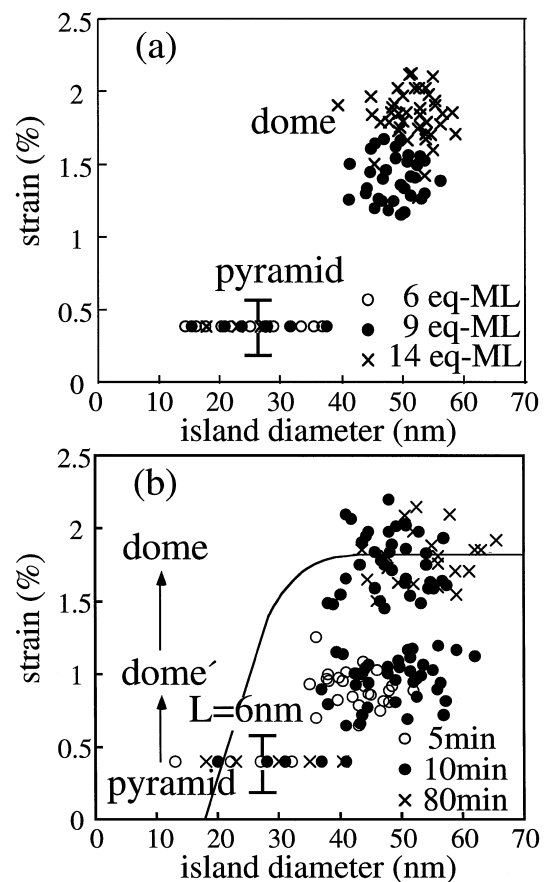


FIG. 2. Strain in Ge islands vs island diameter. (a) For as-deposited samples 6, 9, and 14 eq-ML thick grown at 600 °C and (b) for 8 eq-ML thick samples deposited at 550 °C and annealed at 550 °C for 5, 10, and 80 min. The error ranges both in diameter and strain are 10%. The solid curve in (b) represents the dependence of the island diameter on the strain of equilibrium islands with isotropic surface energies, derived from the work of Kukta and Freund [17] using  $L = 6$  nm (see text for details). The island populations in a sample annealed for 40 min are similar to that for 80 min (data not shown).

samples deposited at 600 °C [Fig. 2(a)]; and for 5, 10, and 80 min annealing at 550 °C after 8 eq-ML Ge deposition at 550 °C [Fig. 2(b)]. The island diameter is measured on the same strain contrast image and scaled down by a factor of 0.8 and 0.85 for domes and pyramids, respectively, which is calibrated by an off-axial TEM imaging where no other diffraction spots are excited. The off-zone imaging is dominated by the composition and optimized for the diameter measurement of coherent islands. Because strain in pyramids is small and could not be measured accurately below a diameter where there is no first fringe present to either side of an island center, we do not indicate the strain of individual pyramids for all samples. Instead, in Fig. 2 we show the upper and lower limits representing the range of the strain for pyramids. We set the upper limit by the condition that the spacing between the first fringes to either side of the island center is larger than the island diameter. The lower limit is chosen arbitrarily so that the error bar is  $\pm 50\%$ , which is 5 times the accuracy of this technique. Excluding pyramids, the errors both in diameter and strain in Fig. 2 are  $\pm 10\%$ . From Fig. 2(a), the average strain of the domes increases from  $1.4\% \pm 0.2\%$  for 9 eq-ML Ge film to  $1.8\% \pm 0.2\%$  for 14 eq-ML Ge film, and strain saturates at the limiting diameter of 60 nm and 2% strain. During annealing, the average diameter also increases, and the sample annealed for 80 min has a slightly broader diameter distribution of domes than observed in Fig. 2(a). Most notably, the domelike islands annealed at 550 °C form two distinct loci in the diameter-strain scatter plot in Fig. 2(b), with strains centered at 1% and 1.8%, whereas the domes grown at 600 °C reveal two closely spaced groups centered at 1.4% and 1.8% strain. Thus, strain is demonstrated to be an extremely sensitive quantitative parameter for evaluating the state of an island that can supplement size and shape information. The reason is that strain is a function only of shape and not of dimension provided that the effects from edge, corner, and surface stress of islands are relatively small [15–17]. In the following, we correlate the strain information in Fig. 2 to the shape of the evolving islands.

During the deposition experiments at 600 °C [Fig. 2(a)], pyramids are replaced by domes for layers thicker than  $\sim 8$  eq-ML, and the strain increases discontinuously by  $\sim 1\%$  from the largest pyramid to the smallest dome. The strain of the domes increases for the higher Ge coverage sample, suggesting that the aspect ratio increases [18]; this evolution of strain is probably connected with a series of subtle shape changes. While our data clearly reveal that domes can have different strain value, we believe that the dome shapes are not in equilibrium due to the relatively high deposition rate. We also observed the existence of domes with asymmetric facet planes for the as-grown samples, which is further evidence of kinetic limitations. Since the annealing experiments more

closely approach equilibrium conditions, we discuss the relationship between strain and equilibrium island shape for this case in the following.

For the annealing experiments [Fig. 2(b)], we divide the evolving islands into three families, separated by obvious gaps in the strain. Although the strain is scattered over some range for each family, possibly due to a series of subtle shape transitions, we focus only on these three clusters of strain values. Therefore, these three groups of islands represent three shapes, which are pyramids, domes, and the metastable domelike transition shape that was first identified from STM images of Ge islands grown at 600 °C [1]. From an independent study using cross-section TEM (not shown), the shape of the metastable dome is a truncated dome with the sidewall angle that is intermediate between a pyramid and a dome.

Pyramids ( $\pi$ ) and domes ( $\delta$ ) are highly stable shapes, since each has the same saturated strain before transforming to the next shape and persist even after 80 min annealing at 550 °C. Although an equilibrium coverage-strain phase diagram has been calculated using total free energy considerations, this diagram is for a surface that contains only one island shape [4]. The Ge on the Si(001) system is richer and more complex, since this system has two stable shapes with at least one metastable intermediate. We denote this transition island shape as dome' ( $\delta'$ ), in recognition of its metastable nature and resemblance to domes [1]. They disappear rapidly after 15 min annealing at 550 °C, as shown in Fig. 3, where the areal densities of these three types of islands are plotted as a function of the annealing time.

The path for the shape transition of Ge islands on Si(001) is  $\pi \rightarrow \delta' \rightarrow \delta$ . The metastability of  $\delta'$  suggests that the free energy of  $\delta'$  is higher than  $\delta$ . Thus, the rate of the  $\pi$  to  $\delta$  transformation is kinetically limited, since it involves the motion of a large volume of atoms and a relatively large change in surface orientations. The  $\delta'$  shape may correspond to a saddle point [1] or even a local minimum in the activation energy barrier between the two stable shapes. Our finding of this metastable shape is consistent with the existence of a transition shape predicted by Daruka *et al.* [6]. The abrupt change in the strain value from  $\pi$  to  $\delta$  is the fingerprint of a first-order shape transformation.

Next, we compare the theoretical predictions of stable island evolution with size during growth in equilibrium to our experimental results. Kukta and Freund [17] have calculated the shape evolution using continuum mechanics with the assumption of an isotropic surface energy; the equilibrium shapes of islands are approximately hemispherical. The calculations they employ are based on the constant chemical potential condition. They construct a series of equilibrium island shapes as a function of volume.

In the continuum limit, the equilibrium shape of islands is a function of a characteristic length,  $L = \gamma/M\varepsilon_0^2$ , where  $\gamma$  is the surface energy,  $M$  is the plane strain

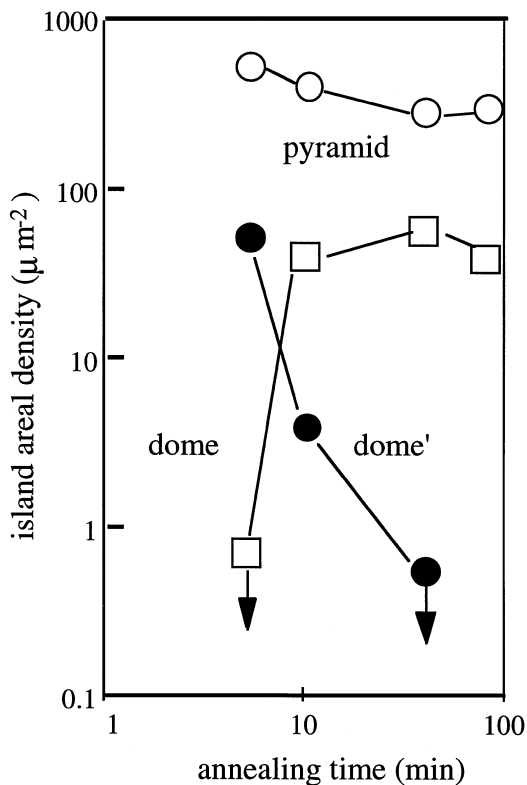


FIG. 3. Evolution of areal densities of pyramids ( $\pi$ ), intermediate shapes ( $\delta'$ ), and domes ( $\delta$ ) as a function of annealing time. The total analyzed area is typically  $0.5 \mu\text{m}^2$ . No domes were observed in a  $1 \mu\text{m}^2$  area for 5 min annealing and no domes' were observed in a  $1 \mu\text{m}^2$  area for 40 min annealing. These upper limits of island density are shown as a symbol with a downward pointing arrow.

modulus, and  $\varepsilon_0$  is the lattice misfit. Since Kukta and Freund analyzed the case of uniaxial strain, we must modify the above equation so that  $L$  can be calculated for the case of biaxial strain. In the biaxial case,  $L$  increases by a factor of  $\sqrt{2}/(1 + \nu)$  [17], where  $\nu$  is Poisson's ratio,  $\nu = 0.27$ . Therefore, using  $\gamma = 1.1 \text{ J m}^{-2}$  [19] and  $M = 1.1 \times 10^{11} \text{ Pa}$  for Ge, we calculate  $L \approx 6 \text{ nm}$ . Converted from their work, we are able to predict the dependence of the equilibrium Ge island size in diameter on the strain at the interface as the solid curve shown in Fig. 2(b). The theoretical strain value in the  $\pi$  regime coincides only with the small pyramids from the experimental data but agrees reasonably well for the  $\delta$  regime.

There are significant discrepancies between the results of our experiment and the theoretical prediction [see Fig. 2(b)]. The stable pyramid distribution extends sideways from one point in this equilibrium curve and also the evolution of island transformations deviates from the equilibrium predictions. These discrepancies are due to the neglect of anisotropy in the surface energy in their model.

The strain relaxation of islands is a sensitive and quantitative property that allows us to unambiguously distinguish island shapes, both stable and metastable, for lattice mismatched growth of coherently strained nanocrystals. Thus, we determine that there are at least three shapes for coherently strained Ge islands on Si(001) prior to formation of dislocated islands, and that at least a metastable  $\delta'$  shape exists between pyramidal,  $\pi$ , and dome-,  $\delta$ , shaped islands. The change in strain among these three different types of islands is discontinuous, suggesting that the shape transformation from  $\pi$  to  $\delta$  is first order.

The authors thank Hewlett-Packard Laboratories' ULSI Laboratory for use of the deposition equipment. The work at UIUC is supported by National Science Foundation Grant No. DMR-9705440. Sample characterization by TEM was carried out in the Center for Microanalysis of Materials, University of Illinois, which is supported by the U.S. Department of Energy under Grant No. DEFG02-96-ER45439. We also thank Dr. P. D. Miller for help in the development of the TEM technique.

\*Email address: chuanliu@uiuc.edu

- [1] G. Medeiros-Ribeiro *et al.*, *Science* **279**, 353 (1998).
- [2] F.M. Ross, J. Tersoff, and R.M. Tromp, *Phys. Rev. Lett.* **80**, 984 (1998).
- [3] V.A. Shchukin *et al.*, *Phys. Rev. Lett.* **75**, 2968 (1995).
- [4] I. Daruka and A.L. Barabasi, *Phys. Rev. Lett.* **79**, 3708 (1997).
- [5] R. Stanley Williams *et al.*, *J. Phys. Chem. B* **102**, 9605 (1998).
- [6] I. Daruka, J. Tersoff, and A.L. Barabasi, *Phys. Rev. Lett.* **82**, 2753 (1999).
- [7] P.D. Miller *et al.*, *Appl. Phys. Lett.* **75**, 46 (1999).
- [8] P.D. Miller, C.P. Liu, and J.M. Gibson (to be published).
- [9] A.J. Steinfert *et al.*, *Phys. Rev. Lett.* **77**, 2009 (1996).
- [10] J.A. Floro *et al.*, *Phys. Rev. B* **59**, 1990 (1999).
- [11] T.I. Kamins *et al.*, *J. Appl. Phys.* **85**, 1159 (1999).
- [12] G. Medeiros-Ribeiro *et al.*, *Phys. Rev. B* **58**, 3533 (1998).
- [13] V.I. Davydov, *Germanium* (Gordon and Breach, New York, 1966).
- [14] Y. Androussi, T. Benabbas, and A. Lefebvre, *Philos. Mag. Lett.* **79**, 201 (1999).
- [15] J. Tersoff and F.K. LeGoues, *Phys. Rev. Lett.* **72**, 3570 (1994).
- [16] L.B. Freund, H.T. Johnson, and R.V. Kukta, *Mater. Res. Soc. Symp. Proc.* **399**, 359 (1996).
- [17] R.V. Kukta and L.B. Freund, *J. Mech. Phys. Solids* **45**, 1835 (1997); (private communication).
- [18] T.I. Kamins *et al.*, *J. Appl. Phys.* **81**, 211 (1997). In these initial AFM studies, the dome height was reported to increase significantly at constant diameter. More recent AFM and STM data have given a significantly more constant dome shape.
- [19] R.J. Jaccodine, *J. Electrochem. Soc.* **110**, 524 (1963).